

The Physics of Pulsations
Gas Machinery Conference 2008

Dennis Tweten
Marybeth Nored
Klaus Brun, Ph.D.

Introduction

The principles of acoustics have been well studied over the last century because of the applicability of acoustic theory to the broad spectrum of noise-related engineering problems. In the design of piping systems for reciprocating compressors in the 1940's and 1950's, the simplest filter designs were derived from basic acoustic theory. Though some of the basic principles may be analogous, reciprocating compressor-induced pulsations are not equivalent to small pressure perturbations described by basic acoustic theory. When modeling and designing reciprocating compressor systems, distinguishing the pulsations as distinctly different from acoustic waves will result in a more accurate depiction of the pulsation amplitudes and the response of the piping system.

This paper compares the mathematical assumptions of the acoustic theory (wave equation solvers) with those of a fully fluid dynamic model. The paper also presents case studies to demonstrate the difference in pulsation predictions between acoustic and full fluid dynamic models. The effect of the full fluid dynamic model on the prediction of pressure peak-to-peak magnitudes, pulsation wave form, and resulting frequency spectrum distributions is discussed. Finally, the paper highlights methods of controlling pulsations from a physics point of view to show why pulsation control methods work to mitigate problematic system frequencies.

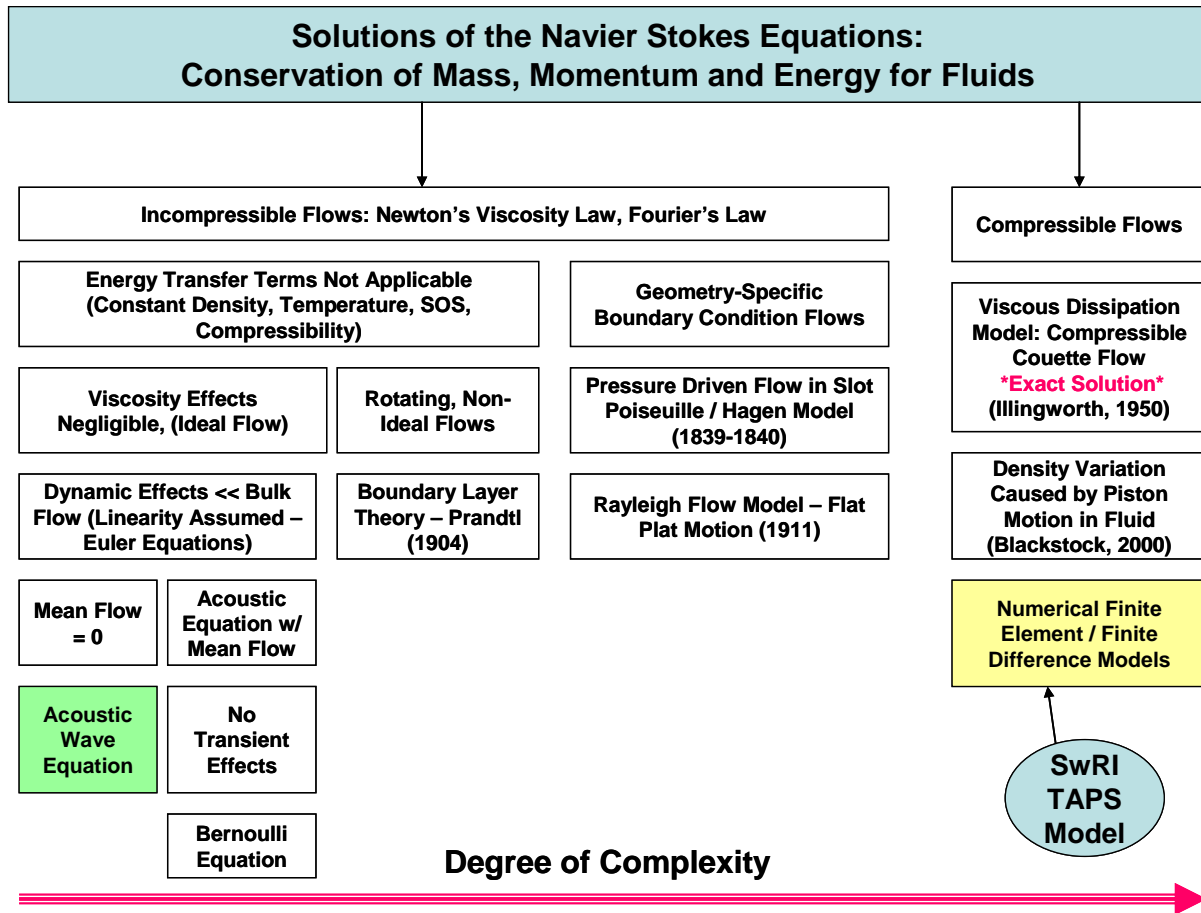
The Fluid Equations

For the last fifty years the compression industry has relied on acoustic analysis tools to determine piping system resonances for reciprocating compressor stations. This was initially accomplished using an analog electric circuit simulation where essential compression station elements were simulated using function generators, resistors, capacitors, and inductors. Namely, the transient acoustic wave equation was simulated based on the functionally identical governing equations of electric circuitry. Later, in the 1990's, this was improved upon by the application digital computer simulations of the transient acoustic equations using numerical solver algorithms. However, both approaches did not solve the actual fluid dynamic equations of pulsating flow in pipes. Instead, the acoustic analysis models solved a linear set of equations derived from the original fluid dynamic equations. These equations were greatly simplified to require no mean through-flow, infinitely small pressure pulsations, no viscosity, and quasi-constant gas properties in order to obtain a solution faster.

Unfortunately, these assumptions also severely limit the method's ability to correctly predict pulsation magnitudes. For variable-speed high-rpm machines, where resonance management is inevitably required, accurate prediction of pulsation magnitudes is critical to compressor station design. Specifically, as pulsations in real piping system are non-negligible portion of the flow stream and the mean flow component is significant, the inertial transport terms and the viscous terms of the governing equations must be included in the analysis to prediction transient dynamic pressures.

The acoustic wave equation is one subset of the fluid dynamic equations which describe mass, momentum and energy transfer in a fluid. These equations are known as the Navier Stokes set of equations. The acoustic wave equation is a convenient description of the conservation of mass and

momentum, which allows for superposition of solutions and a linear solution in time and space. In the same manner that Bernoulli's equation was derived for simple, steady state fluid systems from the more complex Navier Stokes equations, the acoustic wave equation was derived for very small, time-varying perturbations in a fluid. A general diagram of the many fluid solutions to the Navier Stokes equations is shown in Figure 1, to indicate where the acoustic wave equation falls in the class of linear, inviscid, incompressible flow solutions.



Changes to the pressure, density and velocity produced by viscous effects and the variation in the mean flow are not described by the acoustic wave equation. The only method of characterizing these effects is through loss coefficients – which are typically independent of the time wave. This downfall in the acoustic wave description also means that the frequency-dependent loss constants cannot easily be implemented in a classic wave equation solver, although the attenuation of low frequency waves over long distances is significantly less than the attenuation of high frequency (> 200Hz) pressure waves.

Derivation of the Acoustic Wave Equation

To derive the acoustic wave equation, the fundamental conservation of mass and momentum equations are required. As shown in Figure 1 above, the density, viscosity and thermal conductivity terms are assumed constant (and not dependent on thermal energy transfer). Hence, the third Navier Stokes equation is not used in the acoustic wave equation derivation. In addition, the viscous terms are considered negligible and therefore eliminated. In the reciprocating compressor application, a one-dimensional form of the equations is applicable where the velocity, pressure and density terms can be viewed as the sum of two parts: a steady state component and the dynamic component, due to the effect of

the pressure wave produced by the reciprocating compressor. (This view of the equations will help to delineate the non-linear terms and the pulsation-related effects.)

$$\begin{aligned}\rho &= \rho_o + \rho' \\ \vec{U}_{total} &= \vec{U} + \vec{u} \\ P_{total} &= P + p'\end{aligned}$$

The acoustic wave equation will be derived based on a set of assumptions, which do not necessarily apply to the application of high speed reciprocating compressors. The validity of these assumptions will be discussed throughout. The one-dimensional conservation of mass can be examined first. The density and velocity terms are shown with a steady state component and the perturbed component due to the pulsating wave:

$$\frac{d(\rho_o + \rho')}{dt} + \frac{d}{dx}(\rho_o + \rho')(\vec{U} + \vec{u}) = 0$$

The derivative in time and x-direction can be taken for each term, with the assumption that the mean fluid density and mean flow do not vary in space or time. This leaves four specific derivatives in the continuity equation:

$$\rho_o \frac{d\rho'}{dt} + \vec{U} \cdot \frac{d\rho'}{dx} + \rho_o \frac{d\vec{u}}{dx} + \frac{d(\vec{u} \cdot \rho')}{dx} = \rho_o \frac{d\rho'}{dt} + \vec{U} \cdot \frac{d\rho'}{dx} \overset{U=0}{\cancel{}} + \rho_o \frac{d\vec{u}}{dx} + \frac{d(\vec{u} \cdot \rho')}{dx} \overset{Non-linear \sim 0}{\cancel{}} = \rho_o \left(\frac{d\rho'}{dt} + \frac{d\vec{u}}{dx} \right)$$

The second term cancels because the mean flow is assumed to be zero in the acoustic wave equation (which is clearly not the case for the pulsations in the flow stream near a reciprocating compressor). The fourth term is considered negligible for acoustics because the dynamic velocity and perturbation in density due to the pressure wave are very small terms ($\ll 1$) that produce a smaller product. The fourth term will produce a non-linear effect in the pulsation model when it remains in the model. Hence, in the acoustic wave equation model, the continuity equation becomes the product of the variation in density in time and the variation in acoustic velocity with space.

The one-dimensional momentum equation has a similar substitution where the steady and dynamic terms for density, velocity and pressure are substituted. (Viscosity terms are set to zero.) The inviscid momentum equation for only the x-dimension is:

$$\frac{d(\vec{U} + \vec{u})}{dt} + (\vec{U} + \vec{u}) \cdot \frac{d}{dx}(\vec{U} + \vec{u}) + \frac{1}{(\rho_o + \rho')} \frac{d}{dx}(P + p') = 0$$

Distribution of the derivative produces a momentum description with four terms. Again, the mean flow is assumed to be constant in space and time, which reduces the number of terms. The resulting equation (see below) is reduced for the acoustic solution by assuming mean flow is zero (term 2) and that the product of the acoustic velocity and its variation in space is negligible (term 3). Furthermore, a Taylor series approximation is used because the density fluctuation is assumed to be small (acoustically). This reduces the momentum equation to two terms as well – also known as the linear Euler equation:

(1) The kinematics of the compressor drive, which provides a forcing inlet boundary condition to the piping system. This boundary condition must be applied in the numerical model to approximate the actual pulses generated by the piston and released through the cylinder valves.

(2) The fluid dynamic behavior (response) of the piping system and passive outlet boundary condition. In order to calculate the velocity and the pressure at every point in time in the piping system, the transient one-dimensional incompressible flow Navier-Stokes equations are solved – shown below. The solution depends on the outlet boundary condition applied in the model. Typically, these boundary conditions describe an open bottle (constant pressure), entry into a pipeline (infinite boundary condition), or closed end (velocity equal to zero).

$$\frac{\partial \rho}{\partial t} + \frac{\partial(\rho v_x)}{\partial x} = 0$$

$$\rho \left(\frac{\partial u}{\partial t} + u \frac{\partial u}{\partial x} \right) = - \frac{\partial P}{\partial x} + \mu_s \frac{\partial^2 u}{\partial x^2}$$

In the above momentum equation, the viscosity, μ_s , is the combined viscosity and turbulent eddy viscosity, where the turbulent eddy viscosity is usually determined using a second order Reynolds number based turbulence model. In pipe flow, there are two terms in the momentum equation that include viscosity. Both terms will effect the shape of the pulsating wave as it propagates along the pipe – but in varying degrees depending on the magnitude of the dynamic pressure amplitude.

The first viscosity-related term comes from the second partial derivative of the velocity in the streamwise direction. This term must be handled explicitly. To properly capture the nonlinearity of this term, small time steps and fine grid spacing is required. However, this time step and grid spacing is not smaller than what is required to capture complex wave shapes of high frequency pulsating flow anyway, so this was not found to be a limitation.

The second viscosity-related term represents the second partial derivative in the stream-normal direction. This term can be treated implicitly using basic pipe friction loss coefficients and does not require viscosity directly (only within the context of Reynolds number). The a) term does require viscosity (and turbulence eddy viscosity) directly and must be handled explicitly. The following case studies will refer to both of these viscosity-related losses in the model prediction of the pulse wave.

Pulsations in Piping Systems

The differences between the full Navier-Stokes and the Acoustic Wave Equation can be demonstrated using case studies. Several case studies are presented here to demonstrate the differences in the two equations. Specifically the effects of dynamic velocity and damping in the Navier-Stokes equation are contrasted with the Acoustic Wave Equation which does not contain these terms. The following case studies were run using the TAPS solver with full Navier-Stokes implementation and an equivalent time domain acoustic solver.

Figure 2 illustrates a comparison between the Navier-Stokes equation and the Acoustic Wave Equation for a single strong pulse. The figure shows the difference in the pulse shape at the beginning and end of a 1000 meter long pipe for both the Navier-Stokes solver and Acoustic Wave solver. In this first comparison the initial pulse is identical, although the initial shapes shown have already begun to diverge. As the pulse reaches the end of the pipe the shapes differ greatly as the dynamic velocity term begins to

dominate in the Navier-Stokes Equations. The pulse shape from the Navier-Stokes equation has turned into a shock wave with the pressure building at the leading edge of the wave.

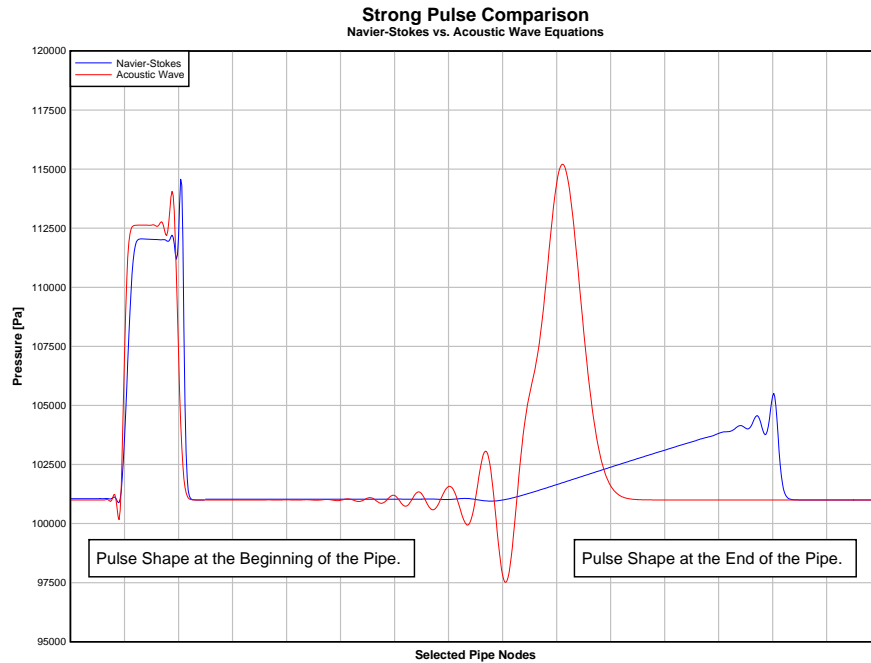


Figure 1. Strong Pulse Comparison.

Figure 2 illustrates a comparison between the Navier-Stokes equation and the Acoustic Wave Equation for a single weak pulse. In this case the pulse has a low enough pressure peak that the dynamic velocity plays a relatively small role in the shape of the pulse. Therefore, the pulse at the end of the pipe for both the Acoustic Wave equation and the Navier-Stokes equations is very similar. The differences shown are most likely due to friction affects.

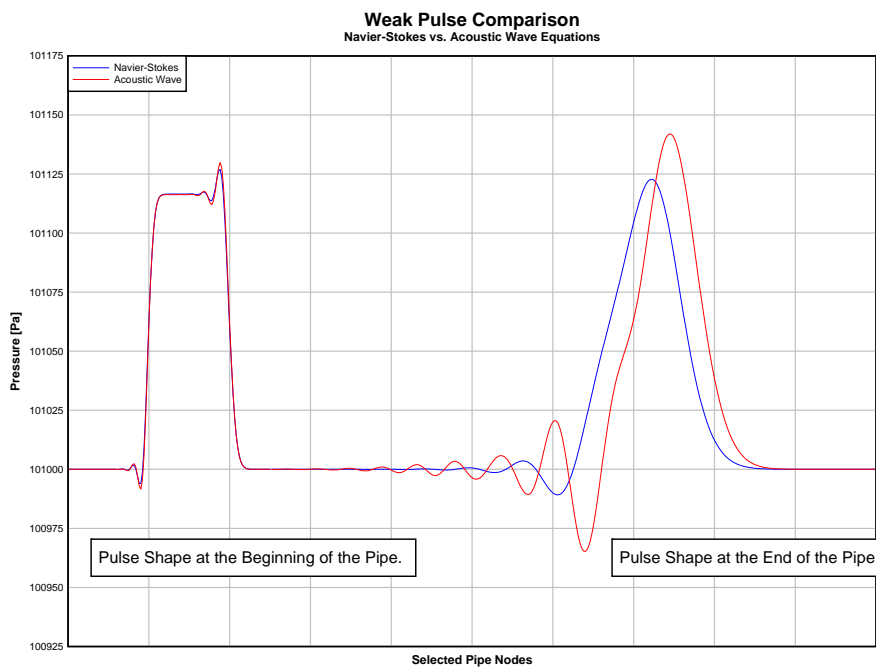


Figure 2. Weak Pulse Comparison.

Figure 3 illustrates the affect of friction in the Navier-Stokes equation that is not present in the Acoustic Wave equation. The figure shows how the amplitude of the sine wave decreases over the length of the pipe for the Navier-Stokes solver. The Acoustic Wave solver and Navier-Stokes without friction affects are also presented on this plot. In both of these later cases the amplitude of the sine wave remains nearly constant.

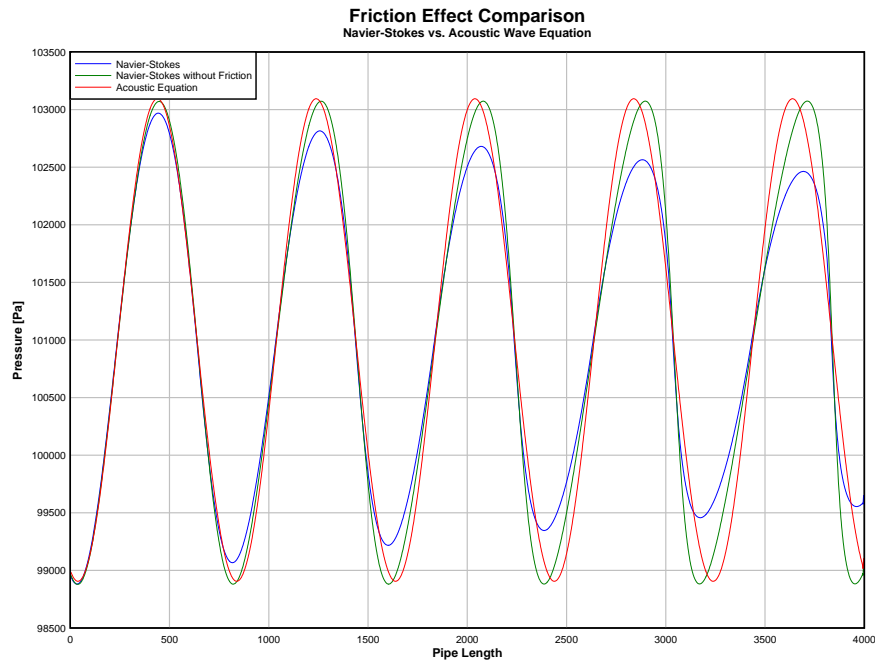


Figure 3. Friction Loss Comparison.

Figure 4 provides a comparison of the Navier-Stokes and the Acoustic Wave solvers for a square wave. A square wave was simulated in a 1000 meter long pipe for this comparison using both the Navier-Stokes and Acoustic Wave equations. The square wave calculated with the Navier-Stokes equation decreases in amplitude due to friction affects and slowly changes shape over the length of the pipe due to dynamic velocity affects. In addition, the mean about which the pulse fluctuates slowly decreases in the Navier-Stokes solution. This decrease is also caused by friction affects due to pressure losses along the pipe. The amplitude of Acoustic Wave solution remains constant over the length of the pipe and the shape of the wave remains constant.

Figure 5 shows the Fast Fourier Transform (FFT) of the square wave solved with both the Acoustic Wave and Navier-Stokes equations for the beginning of the pipe. There is little difference in magnitude or frequency content between the two solutions at the beginning the pipe. Figure 6 presents the FFT of the square wave solved at the end of the pipe with the two equations. As expected the magnitude and the frequency content differ between the solutions. The changes in the Navier-Stokes square wave are due to the friction affects and the dynamic velocity affects along length of the pipe. This particular case shows that both the magnitude and frequency content of a pulsation predicted is different depending on the whether the Acoustic Wave equation or the Navier-Stokes equation is used. In this case the acoustic wave happens to be conservative, but this is not necessarily the rule.

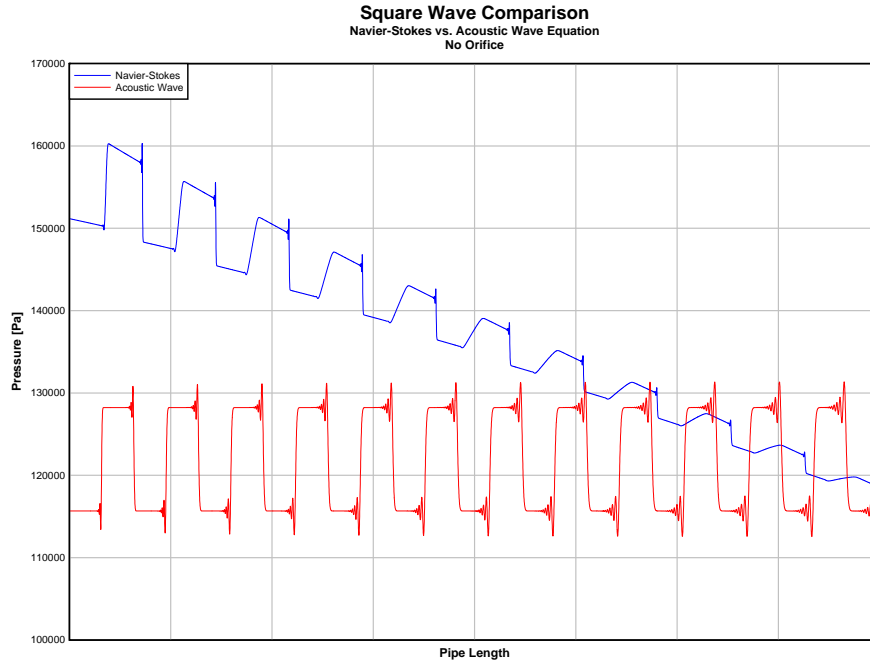


Figure 4. Square Wave Comparison.

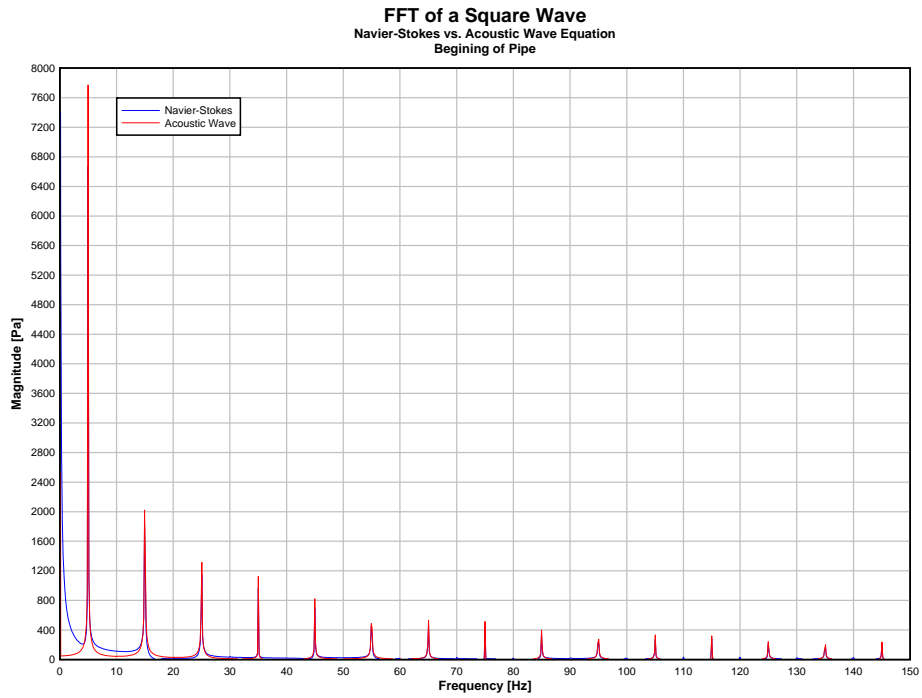


Figure 5. FFT of Square Wave at the Beginning of the Pipe.

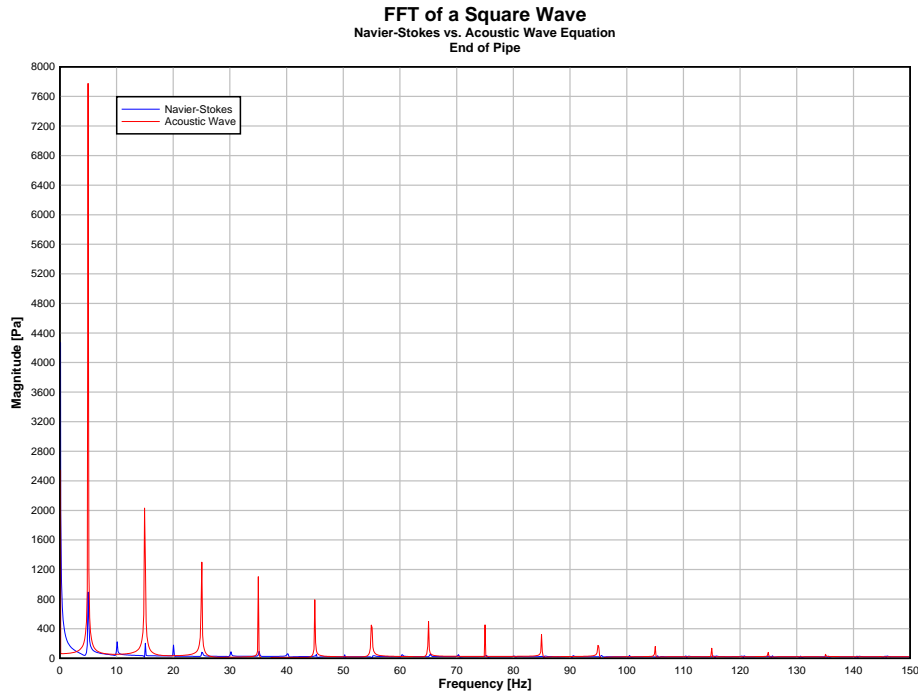


Figure 6. FFT of Square Wave at the End of the Pipe.

Figure 7 provides an additional comparison of the Navier-Stokes and the Acoustic Wave solvers for a square wave. In this case a square wave was simulated in a 1000 meter long pipe with an orifice in the middle of the pipe. Both the Navier-Stokes and Acoustic Wave equations were used to predict the resulting pulsations. The square wave calculated with the Navier-Stokes equation decreases in amplitude due to friction affects and slowly changes shape over the length of the pipe due to dynamic velocity affects. In addition the orifice creates a marked decrease in pulsation in the pipe downstream of the orifice. The mean about which the pulse fluctuates slowly decreases in the Navier-Stokes solution. This decrease is also caused by friction affects due to pressure losses along the pipe. The amplitude of Acoustic Wave solution is reduced slightly downstream of the orifice. Also, it should be noted that the shape of the pulsations differ greatly between the Acoustic Wave solution and the Navier-Stokes solution. However, this change in shape does not appear to make a significant difference in the FFT at the beginning of the pipe.

Figure 8 shows the Fast Fourier Transform (FFT) of the square wave solved with both the Acoustic Wave and Navier-Stokes equations for the beginning of the pipe. There is little difference in magnitude or frequency content between the waves at the beginning the pipe even though the wave shapes differ. Figure 9 presents the FFT of the square wave solved at the end of the pipe with the two equations. As expected the magnitude and the frequency content differ between the solution generated by the two equations. The changes in the Navier-Stokes square wave are due to the friction affects and the changing shape of the wave as it follows the length of the pipe. In addition the magnitude of peaks have been further reduced by the orifice. This case also shows that both the magnitude and frequency content of a pulsation predicted is different depending on the whether the Acoustic Wave equation or the Navier-Stokes equation is used.

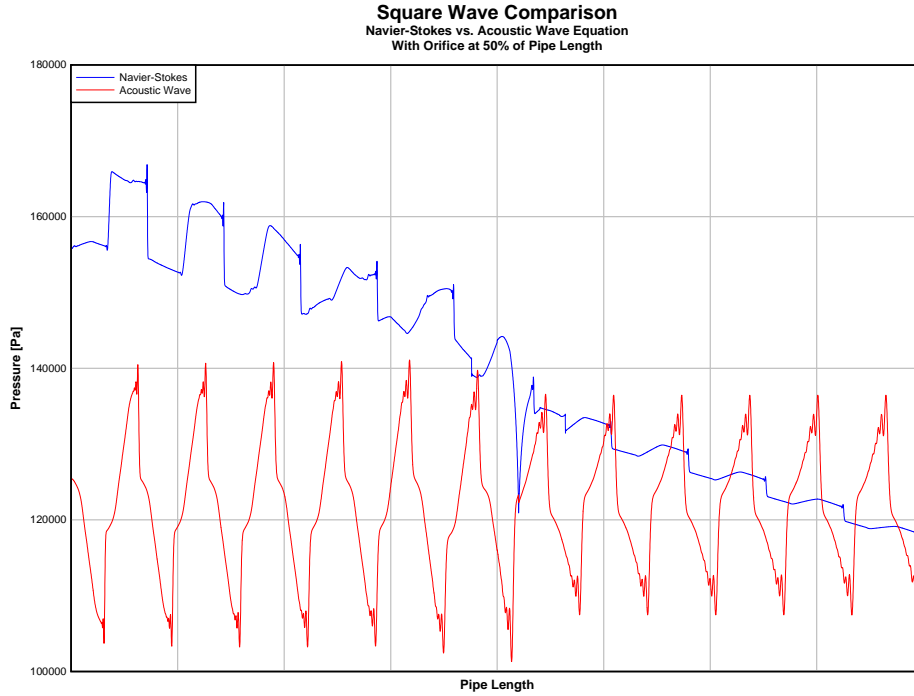


Figure 7. Square Wave with Orifice Comparison.

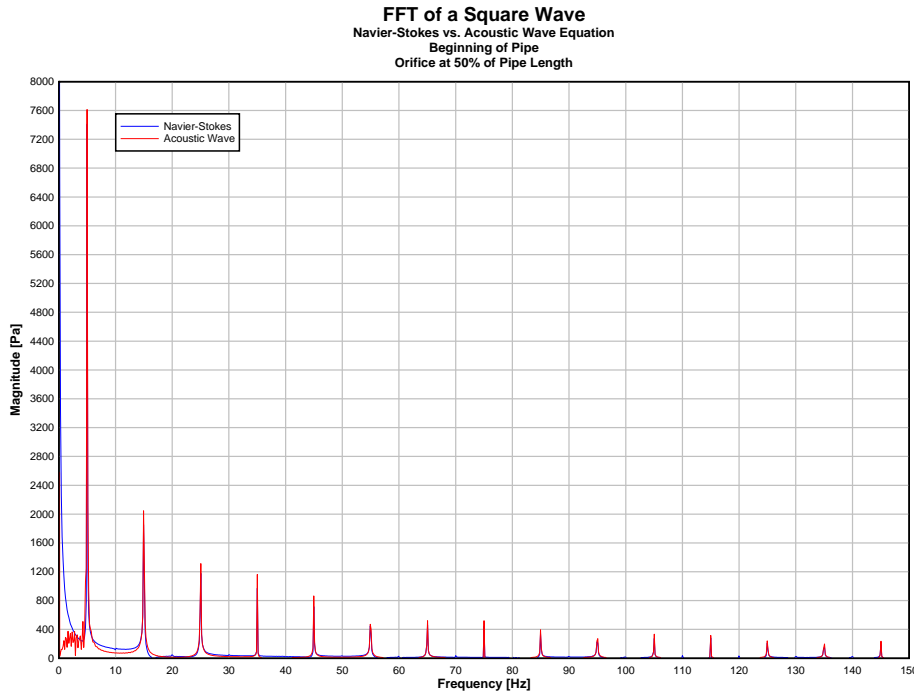


Figure 8. FFT of Square Wave at the Beginning of the Pipe.

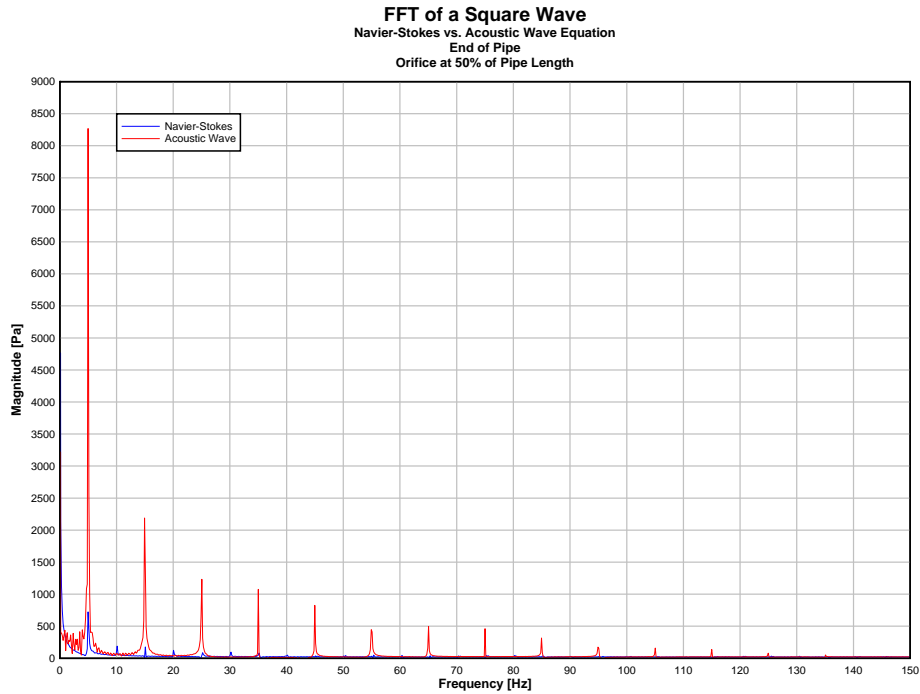


Figure 9. FFT of Square Waves at the End of the Pipe.

Physical Description of Pulsation Attenuation Mechanisms

One of the most important applications of an accurate fluid model of pulsations in a gas piping system is to predict the effect of pulsation attenuation devices in terms of system pressure loss and the reduction of pulsations. Pulsations may be attenuated or reduced through several means (orifice plates, Helmholtz resonators or side-branch absorbers, or volume-choke-volume filters) but physically the various conventional techniques rely on two basic attenuation mechanisms. For the present discussion, the two attenuation mechanisms are referred to as a “choking” effect and a “shifting” effect. The reduction of pulsations in piping systems using traditional pulsation attenuation devices can be explained based on these two physical phenomena.

Attenuation Through Choking

When a pulsating flow stream enters an area reduction, such as an orifice plate, pressure builds up on upstream side of the area restriction. The rise in pressure and corresponding dynamic velocity due to the flow pulse causes the flow through the area restriction to increase proportionally. However, often times the increase in local velocity in the flow particles within the pulse would exceed the speed of sound in the gas stream if this relationship remained proportional. When this occurs, the flow through the area restriction is limited or choked and held to a fixed value of Mach number = 1. This choking effect is illustrated with a basic orifice plate in a pulsating flow stream below.

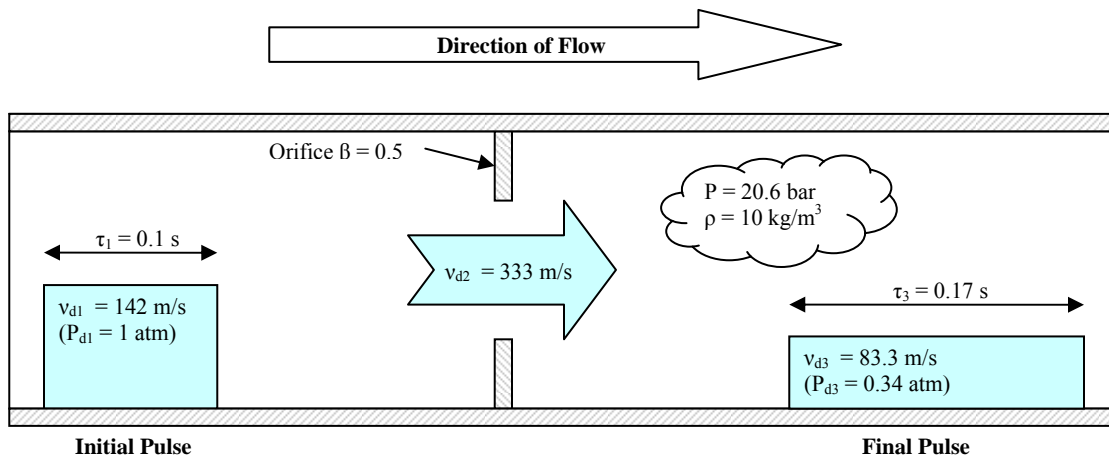


Figure 10. Flow of a Pulse Through an Orifice.

In order to illustrate the choking effect, a typical example is presented in Figure 10. An orifice plate is inserted into a pulsating flow stream near a reciprocating compressor. The amplitude of the pulsations in the flow from a reciprocating compressor can vary from 1 to 50 psi, peak to peak. For the purposes of this example, the pulsation amplitude is set at a low value of 15 psi pk-pk (1 bar). The static pressure is approximately 300 psia (20.6 bar) in the fluid. The flow upstream of the orifice plate possesses a dynamic velocity of roughly 142 m/s corresponding to a pressure increase of 15 psi (1 atm) for the flow pulse, based on a gas density of 10 kg/m^3 (typical for natural gas at 300 psia). When the pulsating flow stream encounters the orifice restriction, the velocity increases in proportion to the area change. Assume the orifice plate beta ratio is 0.5 (which is a typical beta ratio used in pulsation reduction). The area change ratio for the orifice plate is 4:1. For the purposes of this simplistic example, density changes are assumed to be negligible (which is not a valid assumption for high pressure conditions). Then, the flow pulse velocity through the orifice is equivalent to four times the dynamic velocity upstream according to the conservation of mass:

$$\dot{m} = (v_{d1} + v_{s1}) \cdot A_1 \rho_1 = (v_{d2} + v_{s2}) \cdot A_2 \rho_2$$

Since this calculated dynamic velocity in the orifice bore would exceed the speed of sound in the gas stream (nominally $\sim c = 320\text{-}340 \text{ m/s}$), the pressure pulse will be momentarily choked by the area change. Pressure will build up on the upstream side of the orifice plate and elongate the pressure pulse on the downstream side of the plate. This choking effect will also result in a lower amplitude pressure. Since the total dynamic velocity is held fixed by the upper speed of sound limit, the downstream velocity in the expanded pipe area will be approximately 25% of the speed of sound for the same beta 0.5 orifice plate ($v_{d2} = c / 4$). The approximate (neglecting viscous effects) value of the dynamic pressure can be calculated based on the downstream density and reduced dynamic velocity as:

$$P_{d3} = \frac{1}{2} \rho \cdot v_{d3}^2$$

Since the pressure increase will tend to accumulate and the downstream pulses will tend to overlap if the choking effect is too pronounced, there will be a minimum beta ratio for a particular operating condition. Beta ratios smaller than this minimum ratio will have detrimental effects on the downstream pulsations and upstream pressure. This minimum beta ratio allows the maximum increase in

downstream pulse width before the pulses begin to overlap. The net effect on a set of flow pulses traveling through an area restriction is shown below in Figure 11.

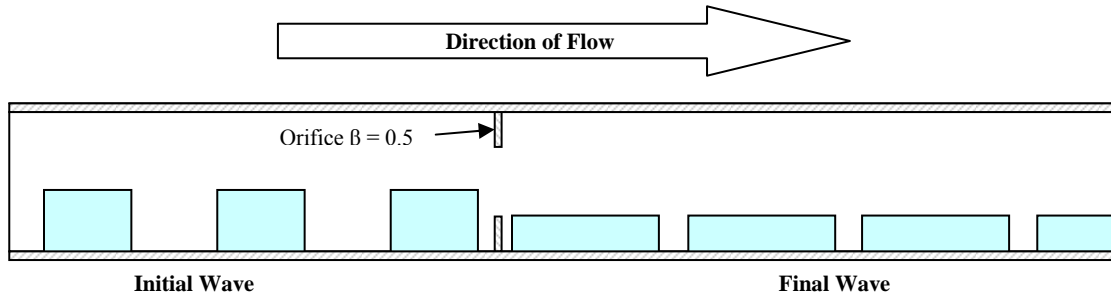


Figure 11. Pulsations Through an Orifice.

It should be noted that it is possible to calculate the ideal beta ratio for a given operating condition and pressure wave amplitude based on fixing the lower limit at the point where the first pressure pulse starts to overlap downstream with the second pressure pulse. In the above example the period of the downstream pulsations was not large enough for the pulsations to overlap so the minimum Beta ratio was not achieved in this case. Any reduction in beta ratio below the lower limit will only produce additional pressure (horsepower) losses without the additional benefit of pulsation attenuation. In addition, for some cases where the pressure pulse amplitude is low and the area restriction is slight, the choking effect will not occur and the attenuation will not follow this behavior.

Attenuation Through Shifting

The second physical means of reducing pulsations is through a shifting effect. This occurs when a portion of the pulsating flow stream is diverted to a closed end in the piping system, which can be either a short stub (side-branch) or a more elaborate closed end achieved through a side branch volume (Helmholtz resonator). Figure 12 below shows a set of pulses traveling down a piping system and splitting into two lower amplitude sets (assuming equal pipe flow areas at the tee intersection). The pulses in the stub branch travel down the length of the branch and then reflect back against the closed end. For the purposes of the example, the stub branch has a length equal to the one-fourth of the wavelength.

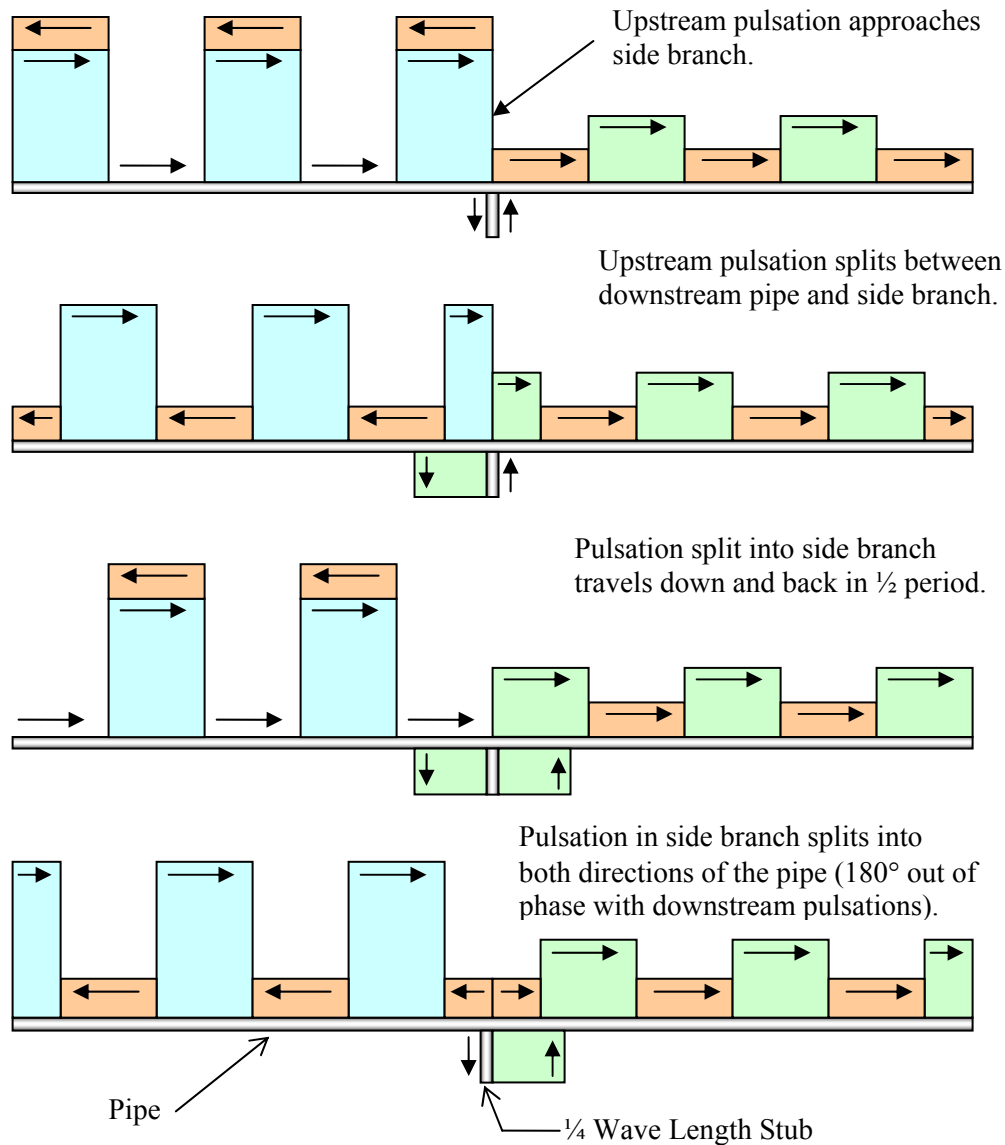


Figure 12. Pulsations Through a Pipe with a Side Branch Attenuator.

When the reflected pulse rejoins the flow stream, its phase has effectively shifted over one complete cycle. This results in tuning out the frequency corresponding to $f = \frac{c}{4 \cdot l}$. The shifted pulsation will create a new or higher amplitude pulse at a different frequency, upstream of the pipe stub. The higher frequency will depend on how the original pulsating flow stream combines with the reflected pulses coming out of the pipe stub. Although the pipe stub has beneficially reduced a particular frequency by shifting the energy to a different frequency, it may cause other resonance conditions to occur. These are often difficult to predict without advanced fluid models which capture the true behavior of the pulsating flow stream.

This effect can also be obtained by doubling the length of the side-stub to create a u-bend geometry. The same shifting effect occurs based on the length of the u-bend. While a specific frequency may be tuned out by this method, the piping in the u-bend will have additional piping losses and other less beneficial effects can be created (downstream pulses traveling through the u-bend in the opposite direction, other resonant conditions at the shifted frequencies, etc.) The u-bend will result in creating a full standing wave condition that typically possesses high vibrations due to this near-ideal resonance condition, as shown in Figure 13 below.

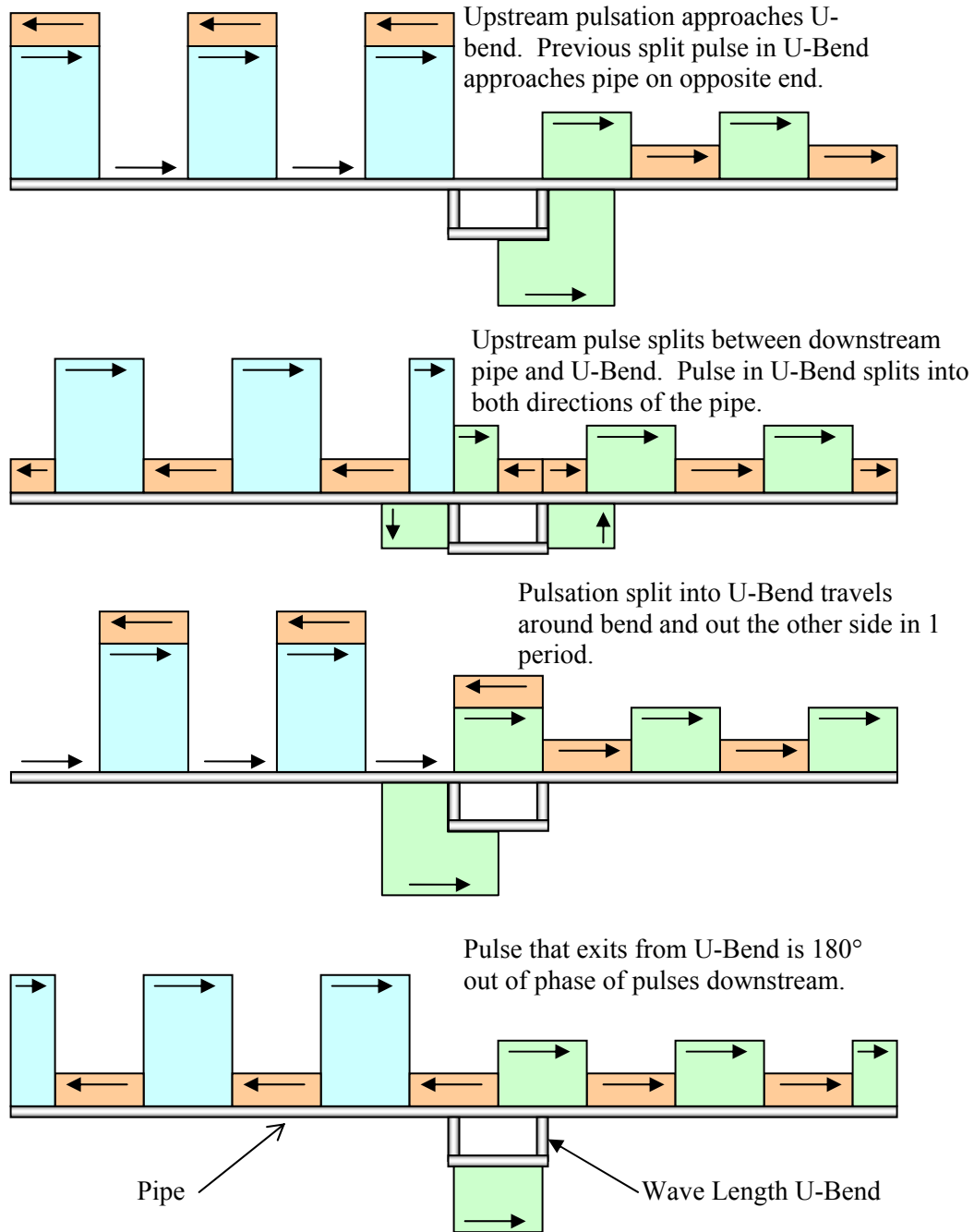


Figure 13. Pulsations Through a Pipe with a U-Bend Attenuator.

Finally, the shifting effect is also used in Helmholtz resonators, though the mode shape is more complicated in this case. The volume-choke geometry allows the pulsation attenuation to be accomplished in a smaller space than a side-branch stub. The classic Helmholtz resonator absorbs a particular frequency corresponding to the Helmholtz equation. In reality, the pressure pulse is shifted to a different point in time when it leaves the volume of the resonator. This effectively produces side bands on either side of the resonator primary frequency due to the shifted pulse.

Summary

In order to overcome the limitations of the acoustic wave equation and more accurately describe the behavior of pulsations, SwRI developed a full one-dimensional time-domain flow solver, named TAPS. This solver includes all terms of the governing fluid equations including fluid inertia, diffusion, viscosity, and energy dissipation. The examples presented here illustrate that both the magnitude and frequency content of pulsations differ significantly in the Acoustic Wave equation and the Navier-Stokes solution. Although many techniques exist for controlling pulsations in the compressor manifold and piping system, the primary attenuation mechanisms can be reduced to physical phenomena, achieved through either choking or shifting of the pulsating flow stream or some combination of these two effects.

References

1. Kinsler, Lawrence E., Frey, Austin R., Coppens, Alan B., Sanders, James V., **Fundamentals of Acoustics, 4th Edition**, John Wiley and Sons, 1976.
2. Panton, Ronald L. **Incompressible Flow, Third Edition**, John Wiley and Sons, 2005.
3. Fletcher, C. A. J., 1988, **Computational Techniques for Fluid Dynamics, Volume I**, 2nd Edition, Springer-Verlag, London
4. Machu, G., 2004, "Calculating Reliable Impact Valve Velocity by Mapping Instantaneous Flow in a Reciprocating Compressor," GMRC Gas Machinery Conference, Albuquerque, New Mexico.
5. Miller, R. W., 1989, **Flow Measurement Engineering Handbook**, 2nd Edition, McGraw-Hill, New York, New York.
6. Colebrook, C. F., 1938-1939, "Turbulent Flow in Pipes, with Particular Reference to the Transition Region Between the Smooth and Rough Pipe Laws," Journal of the Institution of Civil Engineers, London, **11**, pp. 133-156.
7. Fox, R. W. and McDonald, A. T., 1992, **Introduction to Fluid Mechanics**, 4th Edition, John Wiley & Sons, Example Problem 8.8, pp. 366-367.